

^{55}Mn NMR spectrum in a noncollinear antiferromagnet RbMnBr_3

Aleksey M. Tikhonov

Department of Physics, University of Illinois at Chicago, 845 West Taylor Street, Room 2236, Chicago, Illinois 60607

Sergei V. Petrov

P.L. Kapitza Institute for Physical Problems of RAS, Kosygina 2, Moscow 117 337, Russia

(Received 6 December 1999)

The NMR spectrum of ^{55}Mn in an easy-plane noncollinear antiferromagnet RbMnBr_3 was investigated in the frequency range from 380 MHz to 470 MHz under applied magnetic field H up to 85 kOe at $T = 1.3$ K. The NMR spectrum in the noncollinear commensurate phase can be explained by a plane magnetic structure with eight manganese spins per magnetic unit cell. In the collinear phase the NMR frequencies are strongly field dependent. In the vicinity of the critical fields, we observed NMR signals when the radio-frequency field was parallel to the applied magnetic field.

Early neutron diffraction experiments of Glinka *et al.* (Ref. 1) have established that the compound RbMnBr_3 is a noncollinear antiferromagnet at temperatures below $T_N = 8.5$ K. More recent neutron scattering studies^{2,3} showed that the magnetic (H - T) phase diagram consists of several collinear and noncollinear phases. The analyses of the diffraction data were based on the assumption that the RbMnBr_3 crystal has hexagonal symmetry. The results were not unambiguous. For example, according to Ref. 3, at temperatures $T \ll T_N$ and in magnetic fields from 30 kOe to 40 kOe the antiferromagnet has a noncollinear commensurate structure similar to the six-sublattice structure of the hexagonal antiferromagnet CsMnBr_3 .⁴ For the same region of the phase diagram in Ref. 2 RbMnBr_3 was proposed to have a spin structure with a very large unit cell.

An incommensurate spin structure in RbMnBr_3 in the absence of the field has been attributed to uniform orthorhombic distortions in RbMnBr_3 (Refs. 5 and 6). The row model used by Zhitomirsky *et al.* (Refs. 7 and 8) explained the transition from an incommensurate to a commensurate 120° structure. Nevertheless, it did not explain entirely the diffraction pattern observed in the high-resolution neutron scattering experiments (Refs. 2 and 3).

Recently, Petrenko *et al.* (Ref. 9) had carried out an x-ray investigation of a crystallographic structure of RbMnBr_3 at low temperatures. The study showed that the crystal lattice has orthorhombic symmetry in the magnetically ordered state. The symmetry of the charge density distribution restricts the possible variety of magnetic structures that can be realized in the crystal (see, for instance, Ref. 10). Obviously, spin structures with hexagonal space symmetry cannot appear in RbMnBr_3 . Recognizing this fundamental fact, we decided to learn more about the magnetic ordering in RbMnBr_3 and carried out a ^{55}Mn NMR investigation of the antiferromagnet.

The NMR spectrum of ^{55}Mn in an applied magnetic field in a magnetically ordered state of the crystal contains direct information about the number of sublattices in the magnet and orientation of the sublattices relative to each other and to the external field. Using the NMR method in ^{55}Mn nuclei,

we have already observed the distortions in the triangular spin lattice of the noncollinear antiferromagnet CsMnBr_3 (Ref. 11) induced by the magnetic field and a new type of relativistic distortion in a spin structure of the noncollinear antiferromagnet CsMnI_3 .^{12,13} Here we present our results about the fine details of the magnetic structures in RbMnBr_3 at low temperatures ($T \ll T_N$).

RbMnBr_3 crystallizes in a lattice with hexagonal space symmetry $P6_3/mmc$. In the crystal lattice ions Mn^{2+} are surrounded by octahedra of halogen Br^{3+} , and these octahedra, joined at a common face, form chains along the crystal axis C_6 (direction z). The packing of the chains is hexagonal in the basal plane of the crystal. Voids between the chains are filled by Rb^+ . As the temperature decreases, the crystal lattice undergoes structural transformations that are associated mostly with shifts of the chains with respect to each other along the z direction. At temperature $T_{c1} = 470$ K,¹⁴ the crystal lattice undergoes a second-order phase transition to the hexagonal structure $P6_3cm$ with the unit cell increased by a factor of $\sqrt{3} \times \sqrt{3}$ in the basal plane. In this phase one-third of the chains is shifted along the z direction by a small fraction of the crystal period. The first-order phase transition at $T_{c2} = 220$ K (Ref. 15) destroys the hexagonal symmetry. According to Ref. 9, the ion chains are sinusoidally modulated perpendicular to the basal plane. The amplitude of the atomic modulation is small in comparison with interatomic distances in the crystal. Due to distortions of the hexagonal lattice one-fourth of the chains of Mn^{2+} is shifting ‘‘upward’’ along the c axis while another one-fourth shifts ‘‘downward,’’ and the rest remains in the basal plane. The lattice space symmetry is orthorhombic (the space group was not established exactly) with four manganese ions Mn^{2+} per crystal unit cell.

In zero magnetic field ($T \ll T_N$) the magnetically ordered state of the crystal is caused by the spins of Mn^{2+} that are coplanar to a spin plane. The field of the crystal anisotropy orients the spin plane perpendicular to the crystal c axis, which coincides with or is very close to z . The spins form antiferromagnetic chains along c . The exchange interaction between Mn^{2+} ions in the plane is antiferromagnetic. The

spins form a helicoidal structure whose periods in the spin plane are incommensurate with the crystal lattice (Ref. 1). The anisotropy in the spin plane is small (Ref. 16).

If the external magnetic field ($\mathbf{H} \perp c$) is smaller than the exchange field and if $T \ll T_N$, then there are two reorientational phenomena in the H - T diagram of RbMnBr_3 . In a critical magnetic field, $H_{c1} \approx 30$ kOe,^{2,3,16} the incommensurate spin phase transforms into a commensurate noncollinear phase. This phase transition is accompanied by a hysteresis in the intensity and the shape of the antiferromagnetic resonance¹⁷ and simultaneously with small hysteresis in the magnetization curve¹⁶ and birefringence.¹⁸ The commensurate noncollinear phase collapses into the collinear phase in the second critical field H_{c2} , for which $H_{c2} \approx 40$ kOe.¹⁶

Stationary signals of NMR have been excited by a radio-frequency field \mathbf{h} either parallel or perpendicular to the external magnetic field \mathbf{H} . We will show that the NMR spectrum ($\mathbf{h} \perp \mathbf{H}$) in the commensurate magnetic phase does not correspond to the six-sublattice spin lattice.

Monocrystal samples of RbMnBr_3 were grown using Bridgeman method. This procedure was described in detail in Ref. 16. The RbMnBr_3 crystals grown by this method are transparent and can be easily cleaved along binary planes. We have studied five monocrystals prepared at different times.

Experiments were conducted with a wide-range cw NMR spectrometer with a high- Q reentrant resonator and frequency modulation. The design and experimental technique are described in detail in Ref. 11. Most of all the experiments were carried out at $T = 1.3$ K in a field range up to 85 kOe. The magnetic field was applied in the spin plane of the antiferromagnet RbMnBr_3 . The frequency range from 380 MHz to 470 MHz was covered by one split-ring resonator in which polarization of the radio-frequency field (rf field) \mathbf{h} was perpendicular with respect to \mathbf{H} and by one resonator with the polarization $\mathbf{h} \parallel \mathbf{H}$. The spectra were obtained by passing through a resonance with respect to the magnetic field.

In magnetically ordered state of the crystal, the mean field approximation predicts the following dependence of the NMR frequency ω_n of nuclei ^{55}Mn belonging to the same sublattice upon the effective field:

$$\frac{\omega_n}{\gamma_n} = |\mathbf{H}_{hf} + \mathbf{H}| = H_{hf} \left(1 + \frac{H^2}{H_{hf}^2} - 2 \frac{H}{H_{hf}} \cos \theta \right)^{1/2}, \quad (1)$$

$$\mathbf{H}_{hf} = - \frac{A}{\hbar \gamma_n} \langle \mathbf{S} \rangle,$$

where $A < 0$ is the hyperfine interaction constant, $\langle \mathbf{S} \rangle$ is the average ion spin, \hbar is Planck's constant, $\gamma_n/2\pi = 1.06$ MHz/kOe is the gyromagnetic ratio for nucleus ^{55}Mn , and θ is the angle between the external magnetic field vector and the sublattice magnetization.

At liquid helium temperatures the correlations between nuclear and electron motions may become significant due to low-frequency electron spin resonance modes. In this case the NMR spectrum deviates from Eq. (1) and has a strong dependence upon the temperature. This effect is referred to as pulling (Refs. 19 and 20) or as a dynamic frequency shift.

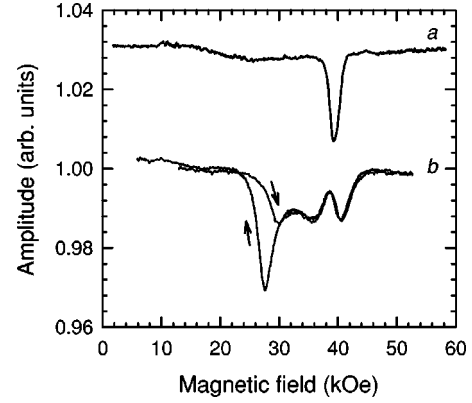


FIG. 1. Examples of recordings of absorption in the antiferromagnet RbMnBr_3 at $T = 1.3$ K: (a) at frequency 390.3 MHz, $\mathbf{h} \parallel \mathbf{H}$; (b) at frequency 439.0 MHz, $\mathbf{h} \perp \mathbf{H}$.

Intensities of NMR signals in magnetically ordered materials are determined by the coefficients of the rf-field gain (see, for instance, Ref. 21). Thus, the quantum resonance transitions of nuclear spins are mostly induced by dynamic components of hyperfine fields.

In the vicinity of the critical field H_{c2} of the collapse of sublattices, even a weak longitudinal rf component in the applied magnetic field is capable of swinging electron spins. As a result, strong perpendicular components of the hyperfine fields appear at the same frequency as that of the pumping rf field. Therefore we were able to observe NMR signals in RbMnBr_3 at rather exotic conditions when \mathbf{h} was parallel to the applied magnetic field. A recording of the magnetic field scan ($\mathbf{h} \parallel \mathbf{H}$) at pumping frequency 390.3 MHz is presented in Fig. 1(a). Absorption was detected in the vicinity of both critical fields H_{c1} and H_{c2} . At these conditions the NMR spectrum in the range of frequencies from 380 MHz to 460 MHz consists of two almost field-independent resonances near H_{c1} and H_{c2} . In the small range of fields that corresponds to the collapse of the noncollinear commensurate phase, the nuclear resonance was especially strong. In CsMnBr_3 , at the same experimental conditions, we observed²² NMR in the interval of fields from $0.8H_c$ to H_c ($H_c \approx 64$ kOe is the field of collapse of the ‘‘triangular’’ phase²³).

When $\mathbf{h} \perp \mathbf{H}$, the rf-field gain coefficient appears because of the joint rotation of the electron spin system in the spin plane. The spectrum of antiferromagnetic resonance in RbMnBr_3 was studied in Refs. 17 and 7. Corresponding to these spin motions, the frequency of the branch of the antiferromagnetic resonance is too high (more than 45 GHz) to distort significantly the NMR frequencies,²⁴ and the spectrum is described by the approximation (1). The experimental spectrum at these conditions is represented in Fig. 2, which contains direct information about the magnetic structure.

Using a method of passing through the resonance with respect to the magnetic field we did not detect absorption at $H < H_{c1}$. Two regions of the rearrangement of the NMR spectrum ($\mathbf{h} \perp \mathbf{H}$) correspond to the critical fields $H_{c1} = 27$ kOe and $H_{c2} = 42$ kOe. The absorption near H_{c1} has hysteresis both in intensity and position of the resonance. This phenomena is demonstrated in Fig. 1(b).

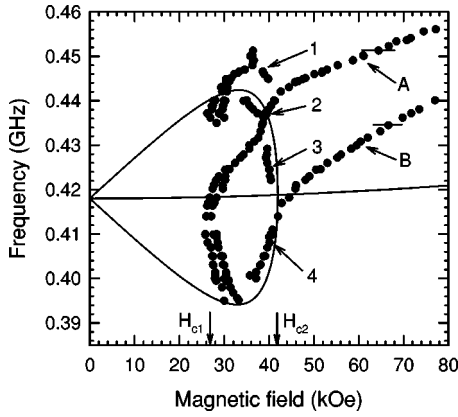


FIG. 2. The NMR spectrum of the antiferromagnet RbMnBr_3 at $T=1.3$ K (dots). Solid lines illustrate the collapse of the triangular spin structure in the mean field approximation (see text).

The NMR spectrum in the noncollinear commensurate phase consists of two pairs of branches (1,2) and (3,4) that merge pairwise in the critical field H_{c2} . In the collinear phase ($H > H_{c2}$), the NMR spectrum consists of two branches A and B that both have a strong dependence of the frequency ν on the magnitude of the applied magnetic field. The value $d\nu/dH \approx 0.5$ MHz/kOe is much greater than follows from Eq. (1) at fixed hyperfine field H_{hf} . The integral intensity of the A branch is approximately the same as the intensity of the B branch.

The magnitudes of H_{c1} and H_{c2} are very well in agreement with the values known from measurements of magnetization,¹⁶ neutron diffraction,^{2,3} and the recent study of the specific heat.²⁵ All samples of RbMnBr_3 had the same NMR spectrum.

The destruction of triangular spin structure on a hexagonal lattice by magnetic field in the mean field approximation was considered by Chubukov (Ref. 26). This rough model qualitatively describes NMR in the hexagonal antiferromagnet CsMnBr_3 . To demonstrate the dramatic difference between the magnetic structure of the commensurate noncollinear phase of RbMnBr_3 and the triangular spin structure we draw in Fig. 2 by solid lines the spectrum for the latter structure. We used formulas from Ref. 11 with the value of exchange field $H_E = 1200$ kOe,¹⁶ critical field $H_c = 42$ kOe, and NMR frequency in zero field $\omega_{n0}/2\pi = 418$ MHz. The experimental spectrum of the noncollinear commensurate phase of RbMnBr_3 is qualitatively different from these dependencies since it contains four branches instead of three.

This discrepancy can be explained by the more complicated spin structure in this phase of RbMnBr_3 . It is represented by a plane structure in Fig. 3 and consists of eight sublattices. In this picture, the magnetic field is applied along the axis o . When the value of H increases, angles α and β decrease to zero, and the collinear phase is realized at H_{c2} . The critical field H_{c1} is very close to H_{c2} , and the angles α, β depend strongly upon the external magnetic field.

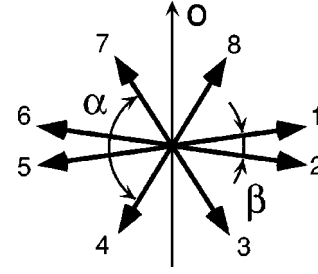


FIG. 3. The magnetic structure in the noncollinear commensurate phase of the antiferromagnet RbMnBr_3 .

The dynamic interaction between nuclei and electrons lifts the double degeneration of the NMR spectrum branches, which is present in the approximation (1), for the proposed structure. The dependence of rf-field coefficients values on the relative orientation \mathbf{h} and \mathbf{H} imposes constraints on the observation of the NMR modes. Four of them we have observed when $\mathbf{h} \perp \mathbf{H}$; the others should be seen at $\mathbf{h} \parallel \mathbf{H}$. Unfortunately, since the gain coefficient drops down too fast with decreasing H/H_{c2} , we failed to separate all branches at the latter case.

The value of β can be estimated from the difference in NMR frequencies for nuclei of the branches 1 and 2, that is, $\Delta\omega_n/2\pi \approx 15$ MHz at $H = 35$ kOe. From the expression (1) $\beta \approx \Delta\omega_n/H\gamma_n \approx 20^\circ$. The same analysis for branches 3 and 4 shows that α at 35 kOe is approximately 120° . Angle β is small and the spin configuration is close to the 120° triangular spin structure.

In addition, using Eq. (1) ($A = -1.51 \times 10^{-18}$ erg from Ref. 27), we have found the average spin of Mn^{2+} for sublattices 1–4 to be $\langle S \rangle' \approx 1.9$ and for 5–8 to be $\langle S \rangle'' \approx 1.8$. All these values are strongly reduced in comparison with quantum number $S = 2.5$ for a free Mn^{2+} ion.

Spin structure in the collinear phase can be described by two types of magnetically nonequivalent chains of Mn^{2+} spins. The strong dependence of the NMR frequencies upon the applied field can be associated with quasi-one-dimensional nature of the exchange interaction in RbMnBr_3 (Ref. 1). From the point of view of the microscopical model,^{28,29} the increase of the NMR frequencies can be interpreted as a suppression of quantum fluctuations by a magnetic field.³⁰

The appearance of the spin structure with eight sublattices in the noncollinear commensurate phase corresponds completely to the crystal structure of RbMnBr_3 at low temperatures. In the commensurate noncollinear phase the magnetic unit cell is two times larger than that of a crystal. In the collinear phase the size of the magnetic unit cell reduces to the crystallographic one.

In closing, we sincerely thank Professor L. A. Prozorova and Professor V. I. Marchenko for numerous fruitful discussions. The authors also thank Alexander Roitman.

- ¹C. J. Glinka, V. J. Minkiewicz, D. E. Cox, and C. P. Khattak, in *Magnetism and Magnetic Materials*, Denver, 1972, edited by C. D. Graham and J. J. Rhyne, AIP Conf. Proc. No. 10 (AIP, New York, 1973), p. 659.
- ²L. Heller, M. F. Collins, Y. S. Yang, and B. Collier, Phys. Rev. B **49**, 1104 (1994).
- ³T. Kato, T. Ishii, Y. Ajiro, T. Asano, and S. Kawano, J. Phys. Soc. Jpn. **62**, 3384 (1993).
- ⁴M. Eibischutz, R. C. Sherwood, F. S. L. Hsu, and D. E. Cox, in *Magnetism and Magnetic Materials*, Denver, 1972 (Ref. 1), p. 684.
- ⁵H. Kawamura, Prog. Theor. Phys. Suppl. **101**, 545 (1990).
- ⁶W. Zhang, W. M. Saslow, and M. Gabay, Phys. Rev. B **44**, 5120 (1991).
- ⁷M. E. Zhitomirsky, O. A. Petrenko, and L. A. Prozorova, Phys. Rev. B **52**, 3511 (1995).
- ⁸M. E. Zhitomirsky, Phys. Rev. B **54**, 353 (1996).
- ⁹O. A. Petrenko, M. A. Lumsden, M. D. Lumsden, and M. F. Collins, J. Phys.: Condens. Matter **8**, 10 899 (1996).
- ¹⁰L. D. Landau and E. M. Lifshitz, *Electrodynamics of Continuous Media* (Pergamon, Oxford, 1975).
- ¹¹A. S. Borovik-Romanov, S. V. Petrov, A. M. Tikhonov, and B. S. Dumesh, Zh. Éksp. Teor. Fiz. **113**, 352 (1998) [JETP **86**, 197 (1998)].
- ¹²S. V. Petrov, A. M. Tikhonov, and B. S. Dumesh, Pis'ma Zh. Éksp. Teor. Fiz. **67**, 661 (1999) [JETP Lett. **67**, 692 (1998)].
- ¹³V. I. Marchenko and A. M. Tikhonov, Pis'ma Zh. Éksp. Teor. Fiz. **69**, 41 (1998) [JETP Lett. **69**, 44 (1998)].
- ¹⁴H. Fink and H.-J. Seifert, Acta Crystallogr., Sect. B: Struct. Crystallogr. Cryst. Chem. **38**, 912 (1982).
- ¹⁵T. Kato, K. Yio, T. Hoshino, T. Matsui, and H. Tanaka, J. Phys. Soc. Jpn. **61**, 275 (1992).
- ¹⁶A. N. Bazhan, I. A. Zaliznyak, D. V. Nikiforov, O. A. Petrenko, and L. A. Prozorova, Zh. Éksp. Teor. Fiz. **103**, 691 (1993) [JETP **76**, 342 (1993)].
- ¹⁷I. M. Vitebskii, O. A. Petrenko, C. V. Petrov, and L. A. Prozorova, Zh. Éksp. Teor. Fiz. **103**, 326 (1993) [JETP **76**, 178 (1993)].
- ¹⁸T. Kato, T. Ishimi, K. Machida, T. Matsui, and K. Ito, J. Magn. Magn. Mater. **140-144**, 1777 (1995).
- ¹⁹A. J. Heeger, A. M. Portis, Dale T. Teaney, and G. Witt, Phys. Rev. Lett. **7**, 307 (1961).
- ²⁰P. G. de Gennes, P. Pincus, F. Hartmann-Bourtron, and J. M. Winter, Phys. Rev. **129**, 1105 (1963).
- ²¹E. A. Turov and M. P. Petrov, *Nuclear Magnetic Resonance in Ferro- and Antiferromagnets* (Halsted, New York, 1972) (Russian originals, Nauka, Moscow, 1969).
- ²²B. S. Dumesh, M. I. Kurkin, S. V. Petrov, and A. M. Tikhonov, Zh. Éksp. Teor. Fiz. **115**, 2228 (1999) [JETP **88**, 1221 (1999)].
- ²³B. D. Gaulin, T. E. Mason, M. F. Collins, and J. Z. Larese, Phys. Rev. Lett. **62**, 1380 (1989).
- ²⁴When pulling is small, the shift of NMR frequencies $\delta\omega$ is determined by the following evaluation: $\delta\omega/\omega_n \sim \omega_T^2/\omega_e^2$, where ω_e is the frequency of the antiferromagnetic resonance and ω_T is the value of the gap in an electronic spectrum due to the hyperfine interaction. According to Ref. 11 for a similar compound CsMnBr₃, $\omega_T/2\pi \approx 7.0/T^{0.5}$ GHz.
- ²⁵F. Perez, T. Werner, J. Wosnitzer, H. v. Lohneysen, and H. Tanaka, Phys. Rev. B **58**, 9316 (1998).
- ²⁶A. V. Chubukov, J. Phys. C **21**, 441 (1988).
- ²⁷K. H. Kerklín and G. L. McPherson, J. Phys. C **16**, 6539 (1983).
- ²⁸T. Ohyama and H. Shiba, J. Phys. Soc. Jpn. **63**, 3454 (1994).
- ²⁹M. E. Zhitomirsky and I. A. Zaliznyak, Phys. Rev. B **53**, 3428 (1995).
- ³⁰A. S. Borovik-Romanov, S. V. Petrov, A. M. Tikhonov, and B. S. Dumesh, Pis'ma Zh. Éksp. Teor. Fiz. **66**, 724 (1997) [JETP Lett. **66**, 759 (1997)].